

## Absolute Cross Sections for Inner Shell Ionization by Lepton Impact

Hans Schneider,<sup>1</sup> Ingo Tobehn,<sup>1</sup> Frank Ebel,<sup>1,\*</sup> and Rainer Hippler<sup>2</sup>

<sup>1</sup>Strahlenzentrum der Universität Giessen, Leihgesterner Weg 217, D-35392 Giessen, Germany

<sup>2</sup>Fakultät für Physik, Universität Bielefeld, Universitätsstrasse 25, D-33615 Bielefeld 1, Germany

(Received 4 March 1993)

We report absolute cross sections for *K*- and *L*-shell ionization of silver and gold targets, respectively, by lepton (electron, positron) impact in the threshold region. The experiments were performed at the slow positron source TEPOS facility at the linac of the Strahlenzentrum in Giessen. A different behavior of positron and electron impact near threshold was observed. In comparison with theoretical calculations, our results suggest that the differences between electron and positron impact are mainly caused by the acceleration or deceleration of the incident projectile in the target nuclear field.

PACS numbers: 34.80.Dp, 34.50.Fa

The interaction of an incident projectile with a target atom may give rise to a variety of different elastic and inelastic scattering processes. Ionization of, for example, inner atomic shells by lepton (positron, electron) impact is one of the processes being of fundamental importance for our understanding of collision dynamics. Experimental investigations for electron impact have been reported by many authors (e.g., Ref. [1] and references therein). For positron impact, few *absolute* cross sections have been reported yet; they were restricted to incident energies  $E_0 \geq 100$  keV (i.e.,  $E_0/I \geq 4$ , where  $I$  is the inner-shell binding energy) [2,3]. No differences between positron and electron impact were reported in these former experiments. In this paper we report first *absolute* cross sections for inner-shell ionization by positron ( $e^+$ ) impact in the threshold regime. We compare these results with cross sections for electron ( $e^-$ ) impact which we have measured with the same apparatus. In the threshold region, we expect different cross sections for positron and electron impact for two reasons: the exchange effect (Ex), important in the ionization by electron impact, and the Coulomb effect (C); the latter effect is caused by the projectile-target nucleus interaction and results in a slowing down ( $e^+$ ) or acceleration ( $e^-$ ) of the incident projectile.

Details of the experimental setup have been described before [4]. Very briefly, it consists of the electron accelerator-based slow positron source TEPOS which delivers intense positron beams of about  $6 \times 10^7 e^+/\text{sec}$ . Positrons with kinetic energy of 2 keV were extracted from the source; they were postaccelerated by a suitable high voltage applied to the target [5,6]. For the measurements with electrons, a corresponding gun was installed in the beamline. The incident energy of the projectiles was varied from 30 keV up to 70 keV for positrons and from 12.3 keV up to 75 keV for electrons. The measurements were performed by detecting characteristic x rays resulting from the inner-shell ionization process. A Si(Li) detector was installed perpendicular to the incident beam. As target we used thin silver (950–5000 Å) and gold (800–1000 Å) monolayer foils and gold/silver

(Au 600 Å/Ag 1000 Å, Au 1000 Å/Ag 1800 Å, and Au 1450 Å/Ag 3500 Å on a carbon backing) multilayer foils. The purpose of these multilayer foils was to measure simultaneously the x-ray yield of the Ag-*K* and the Au-*L*<sub>3</sub> lines and to use the Ag-*L* line for normalization (see below). A major problem in the positron experiment is the large background caused by bremsstrahlung and mainly by  $\gamma$ - $\gamma$  annihilation ( $E_\gamma = 511$  keV) which produces pulses in the low energy region of the registered spectra also. A 3 m long solenoid transport system placed behind the target reduced this background; it was held at  $-10$  keV to compensate for the energy loss in the target foil. Typical x-ray spectra, obtained with 50 keV positron or electron impact of a Au/Ag multilayer target, are shown in Fig. 1; it displays mainly the Ag-*L*, Ag-*K*, and Au-*L* lines superimposed on a continuous background. In the case of electron impact, the background is due to bremsstrahlung which can be calculated with fair accuracy.

To obtain the absolute cross sections we have normalized, for incident electrons, the measured intensities  $\dot{N}_l$  in a given x-ray line to the underlying bremsstrahlung intensity  $\dot{N}_b$ ,

$$\sigma_x = \frac{\dot{N}_l}{\dot{N}_b} 4\pi \frac{d^2\sigma_b}{dkd\Omega} \Delta k,$$

where  $d^2\sigma_b/dkd\Omega$  is the doubly differential bremsstrahlung cross section tabulated by Kissel, Quarles, and Pratt [7], and  $\Delta k$  is the given photon interval.

In case of positron impact, the above procedure was prevented by the large background resulting from positron annihilation. To obtain the absolute cross sections for positron impact, we normalized the measured intensities of the Ag-*K* or Au-*L*<sub>3</sub> lines to the simultaneously measured Ag-*L* line. The Ag-*L* shell has a relatively low binding energy of  $I \approx 3.5$  keV (compared to 25.52 and 11.92 keV for the Ag-*K* and the Au-*L*<sub>3</sub> shell, respectively), corresponding in the present measurements to  $E_0/I \approx 10 \dots 23$ ; at these relatively large values of  $E_0/I$ , only minor differences between positron and electron impact may be expected [5,6,8–11]. We confirmed this by

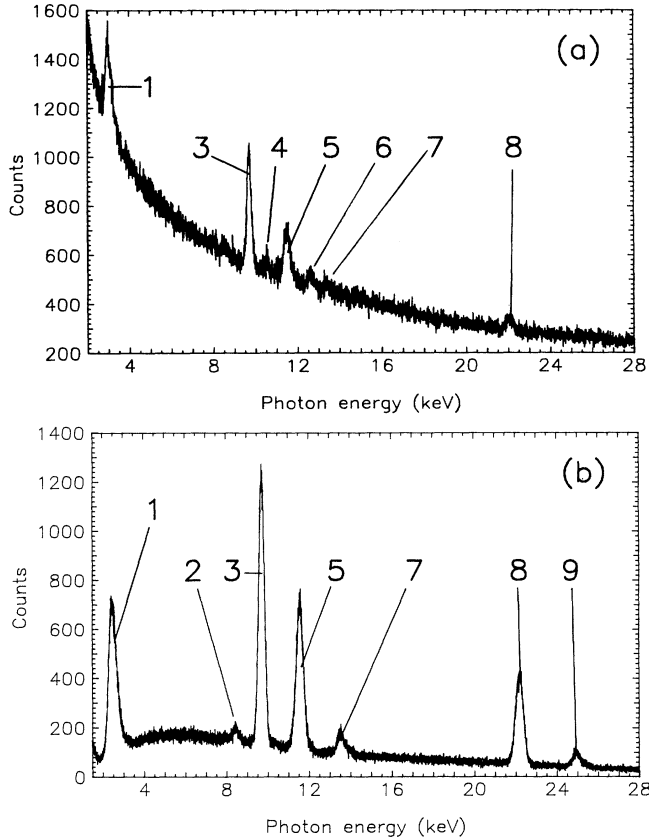


FIG. 1. X-ray spectra from 50 keV positron (a) and electron (b) impact of a Au/Ag multilayer target. Ag-L (1), Au-L<sub>i</sub> (2), Au-L<sub>α</sub> (3), Pb-L<sub>α</sub> (4), Au-L<sub>β</sub> (5), Pb-L<sub>β</sub> (6), Au-L<sub>γ</sub> (7), Ag-K<sub>α</sub> (8), Ag-K<sub>β</sub> (9). Some Pb lines from the lead collimator are also present.

independent calculations performed in plane wave Born approximation (PWBA) in which electron exchange (Ex) and the effect of the nuclear Coulomb (C) field is taken into account [12]. As a result, these calculations yield for the Ag-L shell the cross section ratio  $\sigma_-/\sigma_+ \approx 0.96$  in the energy range of interest here. Using this known ratio together with the absolute cross sections for the Ag-K and the Au-L<sub>3</sub> shell obtained by electron impact enabled us to put the positron data on an absolute scale as well,

$$\sigma_x^+ = 0.96 \frac{\dot{N}_{\text{norm}}^+}{\dot{N}_{\text{norm}}^-} \sigma_x^-,$$

where  $\dot{N}_{\text{norm}}^\pm = \dot{N}_i^\pm / \dot{N}_{\text{Ag-L}}^\pm$  are the corresponding intensities normalized to the Ag-L intensity.

The x-ray cross sections  $\sigma_x$  were converted into the corresponding cross sections  $\sigma_i$  for inner-shell ionization,

$$\sigma_i = \frac{\Gamma}{\Gamma_x} \frac{\sigma_x}{\omega_x},$$

using known fluorescence yields  $\omega_x$  [13,14] and ratios  $\Gamma_x/\Gamma$  of the partial to the total radiative transition proba-

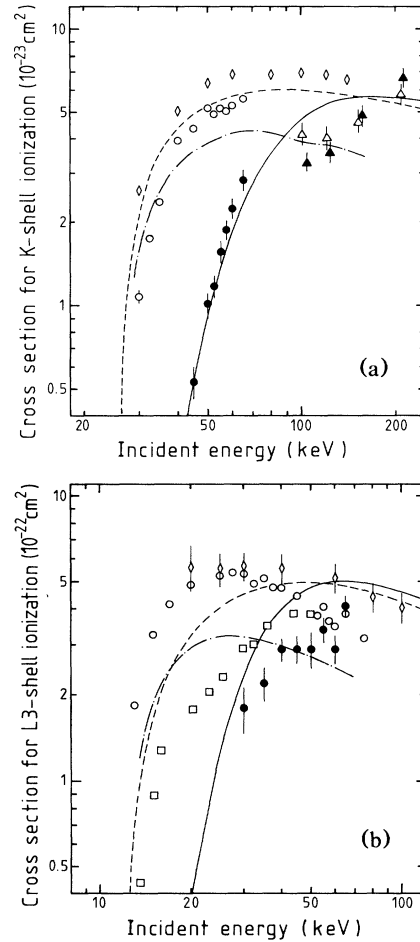


FIG. 2. Absolute cross sections for positron and electron impact of the (a) Ag-K shell and (b) Au-L<sub>3</sub> shell. Present error bars represent statistical uncertainties only. Positron impact: ●, present experimental results; Δ, Hansen and Flammersfeld [2]; —, present PWBA-C calculations. Electron impact: ○, present results; Δ, Hansen and Flammersfeld [2]; ◇, Davis, Mistry, and Quarles [18], corrected for Coster-Kronig transitions; □, Salem and Moreland [19]; ---, present PWBA-C-Ex calculations; - · -, Coulomb-Born-exchange (CBE) calculations [17].

bility [15]. In case of the Au-L<sub>3</sub> subshell, the extracted cross section  $\sigma_{L_3}^i$  had to be corrected for Coster-Kronig transitions describing the nonradiative transfer of vacancies from subshell  $L_i$  to subshell  $L_j$ ,

$$\sigma_{L_3} = \sigma_{L_3}^i - f_{23}\sigma_{L_2} - (f_{13} + f_{12}f_{23})\sigma_{L_1},$$

where  $f_{ij}$  are the corresponding Coster-Kronig factors [14]. The applied correction ( $\sim 20\%$ ) was calculated using theoretical cross sections for  $L_i$ -shell ionization [6]. The accuracy of our results is mainly determined by the accuracy of the normalization procedure, the bremsstrahlung cross sections ( $\sim 10\%$ ), and the fluorescence yields ( $\sim 5\%$ ) and is estimated at  $\pm 25\%$ .

The experimental results for the Ag-K and the Au- $L_3$  ionization cross sections are displayed in Figs. 2(a) and 2(b), respectively. The different threshold behavior caused by positron and by electron impact is perceptible from the present measurements. By contrast, previous experimental investigations for Ag-K ionization performed at larger incident energies between 100 and 400 keV claimed that "no systematic difference has been found" between electron and positron impact [2]; these data also seem to display an incorrect energy dependence [Fig. 2(a)] which may be caused by the relatively thick ( $\sim 50000$  Å) targets used in the previous experiment. As has been mentioned before, differences between positron and electron impact at threshold energies are mainly due to two effects: electron exchange and the Coulomb effect of the target nuclear field on the projectile. Of these two effects, electron exchange is only possible with electron impact and it leads, due to an interference with the direct ionization amplitude, to a *smaller* cross section for electron compared to positron impact. The interaction of the projectile with the nuclear field of the target atom leads to an acceleration or retardation of the incident electron or positron, respectively [16]. Since the incident projectile has to penetrate deep into the target atom to cause ionization of inner atomic shells, it will, depending on its charge, experience an energy loss or gain of the order of the respective binding energy  $I$ . The energy at the instant of the collision with a target electron is about  $E_0 \pm I$  where the  $\pm$  sign corresponds to electron (+) and positron (-) impact. The different energy should cause large differences in the threshold regime where the cross sections display a pronounced energy dependence. These qualitative arguments are confirmed by our own calculations in PWBA which account for the Coulomb effect (PWBA-C) and for electron exchange (PWBA-C-Ex) [6,12]. As it turns out, the exchange effect leads to a decrease of  $\sigma_-$  particularly in the threshold regime; this is more than compensated by the Coulomb effect which dominates in the threshold regime yielding a considerable enhancement of  $\sigma_-$  over  $\sigma_+$ . This theoretical result is in reasonable agreement with our experimental results; for electron impact, this conclusion is further confirmed by Coulomb-Born-exchange (CBE) calculations [17]. Minor discrepancies which are more evident for Au  $L_3$ -shell ionization are presumably due to wave function effects; the calculations have been performed using hydrogenic wave functions which describe the  $L$ -shell less satisfactorily.

In conclusion, our results demonstrate the pronounced sign-dependence of the inner-shell ionization cross section by lepton impact at threshold energies. It is mainly

caused by the Coulomb effect which leads to a drastic decrease (increase) of the respective cross sections for positron (electron) impact.

We would like to thank M. Rückert for valuable assistance and the operating staff of the Giessen linac for technical support. The generous financial support by the Deutsche Forschungsgemeinschaft (DFG) is gratefully acknowledged.

---

\*Present address: Festo Didaktik, Denkendorf, Germany.

- [1] C. J. Powell, Rev. Mod. Phys. **48**, 33 (1976); in *Electron Impact Ionization*, edited by T. D. Märk and G. H. Dunn (Springer, Berlin, 1986), Chap. 6.
- [2] H. Hansen, H. Weigmann, and A. Flammersfeld, Nucl. Phys. **58**, 241 (1964); H. Hansen and A. Flammersfeld, Nucl. Phys. **79**, 135 (1966).
- [3] S. A. H. Seif el Nasr, D. Berényi, and G. Bibok, Z. Phys. **271**, 207 (1974).
- [4] F. Ebel, W. Faust, C. Hahn, S. Langer, M. Rückert, H. Schneider, A. Singe, and I. Tobehn, Nucl. Instrum. Methods Phys. Res., Sect. A **272**, 626 (1988); F. Ebel, W. Faust, C. Hahn, M. Rückert, H. Schneider, A. Singe, and I. Tobehn, Nucl. Instrum. Methods Phys. Res., Sect. B **50**, 328 (1990).
- [5] F. Ebel, W. Faust, C. Hahn, M. Rückert, H. Schneider, A. Singe, and I. Tobehn, Phys. Lett. A **140**, 114 (1989).
- [6] H. Schneider, I. Tobehn, and R. Hippler, Phys. Lett. A **156**, 303 (1991).
- [7] L. Kissel, C. A. Quarles, and R. H. Pratt, At. Data Nuclear Data Tables **28**, 381 (1983).
- [8] S. Ito, S. Shimizu, T. Kawaratani, and K. Kubota, Phys. Rev. A **22**, 407 (1980).
- [9] P. J. Schultz and J. L. Campbell, Phys. Lett. **112A**, 316 (1985).
- [10] W. N. Lennard, P. J. Schultz, G. R. Massoumi, and L. R. Logan, Phys. Rev. Lett. **61**, 2428 (1988).
- [11] U. Schiebel, E. Bentz, A. Müller, E. Salzborn, and H. Tawara, Phys. Lett. **59A**, 274 (1976).
- [12] R. Hippler, Phys. Lett. A **144**, 81 (1990).
- [13] M. O. Krause, J. Phys. Chem. Ref. Data **8**, 307 (1979).
- [14] U. Werner and W. Jitschin, Phys. Rev. A **38**, 4009 (1988).
- [15] J. H. Scofield, Phys. Rev. **179**, 9 (1969).
- [16] M. Gryziński and J. A. Kunc, J. Phys. B **19**, 2479 (1986).
- [17] D. L. Moores, L. B. Golden, and D. H. Sampson, J. Phys. B **13**, 385 (1980).
- [18] D. V. Davis, V. D. Mistry, and C. A. Quarles, Phys. Lett. **38A**, 169 (1972); according to C. A. Quarles (private communication) the published results were not corrected for Coster-Kronig transitions.
- [19] S. I. Salem and L. D. Moreland, Phys. Lett. **37A**, 161 (1971).